AJNR

Functional Localization of Brainstem and Cervical Spinal Cord Nuclei in Humans with fMRI

Barry R. Komisaruk, Kristine M. Mosier, Wen-Ching Liu, Cecily Criminale, Laszlo Zaborszky, Beverly Whipple and Andrew Kalnin

Functional Localization of Brainstem and Cervical Spinal Cord Nuclei in Humans with fMRI

Barry R. Komisaruk, Kristine M. Mosier, Wen-Ching Liu, Cecily Criminale, Laszlo Zaborszky, Beverly Whipple, and Andrew Kalnin

BACKGROUND AND PURPOSE: To our knowledge, no published functional map of the human lower brainstem exists. Our purpose was to use 1.5-T functional MR imaging (fMRI) to visualize the location of cranial nerve (CN) nuclei and other pontine, bulbar, and cervical spinal cord nuclei by using specific sensory stimulation or motor performance.

METHODS: We localized nuclei by using cross-correlation analysis of regional blood oxygen level–dependent (BOLD) signal intensity during specific motor and sensory procedures based on known functions of specific nuclei. Statistical parametric mapping (SPM) analysis was used for comparison. Head, cardiac, and respiratory motion artifact correction was applied. Histologic atlases aided localization.

RESULTS: We obtained evidence of localization of the following nuclei by using tests, as follows: main trigeminal sensory (CN V), brushing the face; abducens (CN VI), left-right eye movement; facial (CN VII), smiling and lip puckering; hypoglossal (CN XII), pushing the tongue against the hard palate; nucleus ambiguus, swallowing; nucleus tractus solitarii (NTS), tasting a sweet-sour-salty-bitter mixture; nucleus cuneatus, finger tapping; and cervical spinal cord levels C1–C3, tongue movement to activate the strap muscles. Activation of cortical motor and sensory areas and somatosensory thalamus corresponded with the tasks and sites of brainstem activation. Head movement was minimal, typically less than 1 mm in all three axes.

CONCLUSION: With 1.5-T fMRI, the CN nuclei of the pons and medulla, and other nuclei of the lower brainstem and cervical spinal cord, can be localized in awake humans with specific sensory stimulation or motor performance.

Although excellent histology-based atlases of the human brainstem exist (1, 2), the Talairach atlas (3), which is commonly used for functional brain mapping, depicts no nuclear groups in the lower brainstem. The present study was designed to ascertain whether current functional MR imaging (fMRI) methods, with a conventional field strength of 1.5 T and the use of a standard head coil, provides adequate sensitivity and resolution to reveal functional activation of specific cranial nerve (CN) nuclei in the medulla oblongata and pons of the lower brainstem in humans.

In the present study, healthy women (n = 4) and men (n = 3) (age range, 22–57 years) were instructed to produce specific voluntary motor patterns as vigorously as was comfortable, or they received selected forms of sensory stimulation, with the objective of activating selected CN and other lower brainstem nuclei. The specific motor and sensory paradigms were selected on the basis of conventional clinical neurologic findings (4–8) supported by recent correlative MR imaging–histologic results (9, 10) and MR imaging–clinical neurologic reports as follows: 1) the abducens nucleus controls left-to-right eye movement (11, 12); 2) the facial nucleus controls the alternating smile-then–lip pucker movement (13, 14); 3) the hypoglossal nucleus controls tongue movement (15–17); and 4) a network that involves the nucleus ambiguus (18, 19) controls the Mendelsohn maneuver, a voluntary prolongation of the elevation of the larynx during swallowing (20–25). (The Mendelsohn maneuver

augments opening of the upper esophageal sphincter; it is a therapeutic maneuver taught to patients with brainstem stroke who have dysphagia.) Perception of specific sensory stimuli requires the integrity of other nuclear regions, as follows: 1) the subject's perception of unilateral brushing of his or her face requires integrity of the trigeminal nucleus (26); 2) perception of a taste mixture (combined sweet, sour, salty, and bitter), the nucleus of the solitary tract (NTS) (27, 28); and 3) perception of finger tapping (ie, afferent activity from the fingers), the nucleus cuneatus (29–31).

Although conventional MR imaging has been used to evaluate lesions of the brainstem (32, 33) and spinal cord (34), reports of the use of fMRI to analyze activity in the brainstem (18–20) or spinal cord (35) are lacking.

The purpose of the present study was to ascertain whether fMRI methods, coupled with performance of specific motor tasks and sensory stimulation, can be used to visualize the specific lower brainstem and cervical spinal cord regions that correspond with the appropriate CN nuclei and other pontine, bulbar, and cervical spinal cord nuclei.

Methods

fMRI Parameters

Individuals underwent imaging in the coronal and sagittal planes by using standard functional MR imaging blood oxygen level–dependent (BOLD) techniques (36) and a 1.5-T MR system. Gradient-echo echo-planar sequences were used, with the following acquisition parameters: 2000/60 (TR/TE); 64 × 64 matrix, 24-cm field of view, 4-mm-thick contiguous sections, and 90° flip angle. For each motor or sensory paradigm, 140 images at each of 14 section locations were obtained by using a standard quadrature birdcage head coil. Coronal images were acquired in a plane parallel to the long axis of the brainstem and cervical spinal cord. Sagittal images were acquired by using a coronal section through the dorsal half of the pons and medulla, which was the localizer. Spin-echo T1-weighted (450/14) high-resolution anatomic images were acquired in the coronal and sagittal planes in the same section locations during the same imaging session. The individual's head was immobilized with foam and taped to the head holder to prevent motion. Institutional approval was obtained, and written informed consent was obtained from all individuals.

Task Paradigms

The individuals performed a series of tasks designed to preferentially activate motor or sensory CN nuclei. Individuals performed the following tasks by using a block paradigm design in which the activity epochs were of 10-second duration and the rest epochs, 30-second duration. Four successive 40-second cycles were performed: 1) tongue tapping, which was self-paced tapping of the tongue against the hard palate, to activate the hypoglossal nucleus (CN XII); 2) alternating smiling and puckering of the lips to activate the facial nucleus (CN VII); 3) self-paced gaze shifting from left to right, in which individuals were instructed to fix their gaze on the vertical bars of the head coil and rapidly shift their gaze from the left to the right, to activate the abducens nucleus (CN VI); and 4) face brushing, in which one of the investigators (K.M.M.) rapidly brushed a cotton swab across the subject's right malar area to activate the trigeminal main sensory nucleus (CN V).

Other tasks involved different epochs of activity and rest and included the following: 1) Finger-tapping was a self-paced bilateral finger-to-thumb apposition task performed for two cycles of 30 seconds on and 30 seconds off (to activate the nucleus cuneatus). 2) The Mendelsohn maneuver was a swallowing task in which the individuals voluntarily prolonged elevation of the hyoid-laryngeal complex (to activate the nucleus ambiguus) for 20 seconds on and 30 seconds off. During the 20-second activity epoch, individuals performed two swallowing cycles in which the hyoid-laryngeal complex was elevated for 3 seconds. 3) In the taste task, individuals self-administered a viscous combination of sweet, sour, salty and bitter agents (ie, sucrose, lemon juice, table salt, and dry mustard, respectively) into the oral cavity through a long flexible plastic catheter. They maintained the mixture in the oral cavity for a period of 60 seconds, alternating with a 60-second epoch in which no substance remained in the mouth (to activate the NTS). Two cycles were performed.

Each subject performed all tasks and underwent all procedures. Validity was ascertained by observing whether BOLD activity systematically varied in relation to the known location of the various nuclear groups in an individual and between individuals. The activity of somatomotor and somatosensory cortex was observed for possible regional (ie, homuncular) correlation with the lower brainstem activation sites. The activity of the somatosensory thalamus was observed for possible correlation with sensory stimuli. The initials of all subjects have been changed in the Figures and Table, to maintain confidentiality.

Data Analysis

Image reconstruction and analysis were performed offline on an UltraSparc 1 workstation by using software routines written in interactive data language (IDL; Research Systems, Boulder, CO). These provided an interface for both cross-correlation analysis and statistical parametric mapping (SPM) analysis. For details of the statistical analysis, please see the Appendix.

For image clarity in a few cases, all pixels in an individual cluster of pixels identified by an arrow were lightened to enhance their contrast when the background was dark. No other modifications to the images were made.

Results

To ascertain whether a particular stimulus or movement paradigm was related to a particular region of activation on the fMRI image, the following procedure was used. Starting with a visualization of all points in brainstem regions that were significantly different ($P \leq .03$), successive displays with increasing stringency (eg, to $P = .0001$) were generated. Thereby, the number of positive points was reduced until the fewest points were observed in the expected brainstem region. The observation of an absence of other positive points in the pons or medulla and a presence of positive points in other regions of the brain, especially cerebellum (eg, Figs 1–8), was common. Thus, the observation of potential false-positive findings (ie, those in regions that are not obviously related to a particular paradigm) in the pons or medulla was far less likely than in other brain regions, such as the cerebellum or cortex.

Each set of stimulus and movement paradigms was applied in each of the seven individuals (two of whom were tested twice). As summarized in the Table, the likelihood of observing activation in the pons and
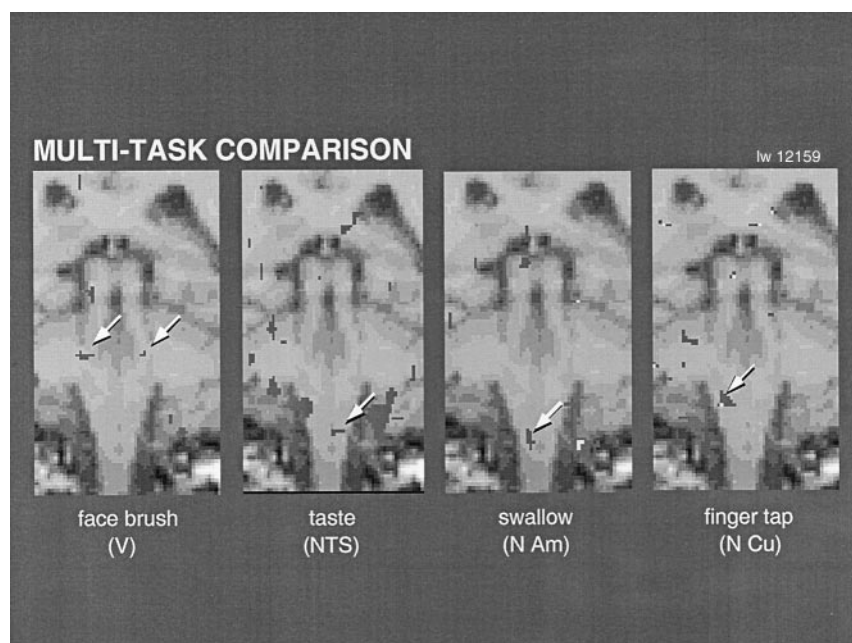
FIG 1. Coronal images obtained with motor tasks and sensory stimuli used to activate different brain regions (*arrows*) in the same individual. These tasks and stimuli correspond to the trigeminal (*V*), solitary (*NTS*), ambiguus (*N Am*), and cuneate (*N Cu*) nuclei.
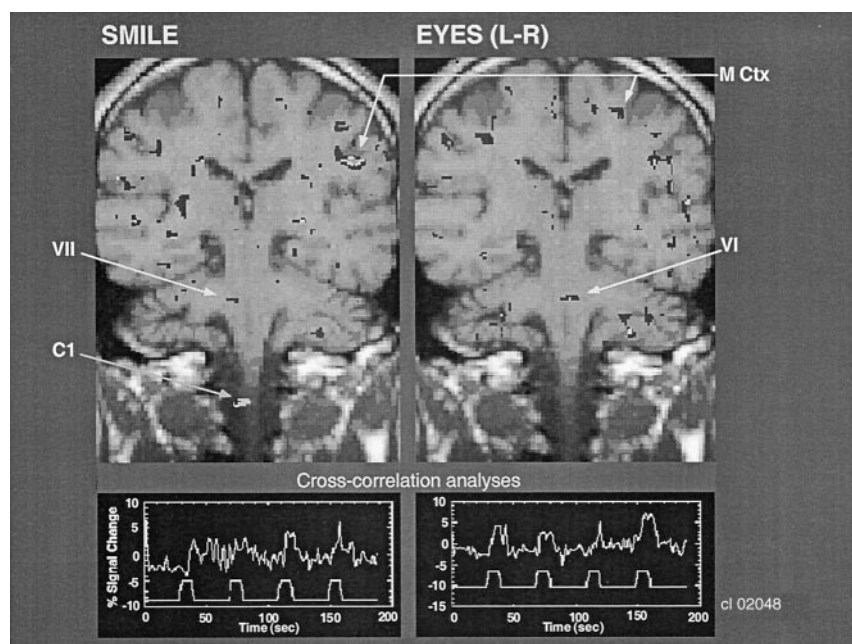

FIG 2. Coronal images show that facial and eye movements activate different adjacent brain regions that correspond to the facial and abducens CN nuclei, respectively. Cross-correlation analysis was performed between the onset and termination of the movements and the BOLD signal change in these pontine regions of activation. *C1* indicates the C1 level of the spinal cord; *M Ctx*, motor cortex; *VI*, CN VI, and *VII*, CN VII.

medulla that corresponded to a particular paradigm ranged from 78% for the nucleus ambiguus (related to swallowing, ie, Mendelsohn maneuver) to 33% for the sensory trigeminal nucleus (related to face brushing). In a preliminary observation, the repeatability of the response was observed in three of six paradigms in subject DD and in one of eight paradigms in subject CL.

Intraindividual Regional Specificity

A semi-diagrammatic representation of the location of brainstem nuclei relevant to the present study is presented in Figure 9. Figure 1 shows a composite comparison of the regions of BOLD activity in the lower brainstem that were observed in a single subject in the same brain section, in relation to the performance of the four sensory and motor tasks. Note the distinctly different regions of activation with each of the tasks.

Figure 2 shows a comparison of the regions of BOLD activity in the same individual in the same brain section obtained with two tasks that involve closely adjacent, but different, CN motor nuclei. The task of alternating between smiling and puckering the lips was correlated with BOLD activation in the region of the facial nucleus (CN VII). By contrast, eye movement (ie, shifting the eyes laterally with alternating left-to-right movement) was correlated with BOLD activation in the pons in the region of the abducens nucleus (CN VI), which provides the motor innervation of the lateral rectus muscles of the eye. The
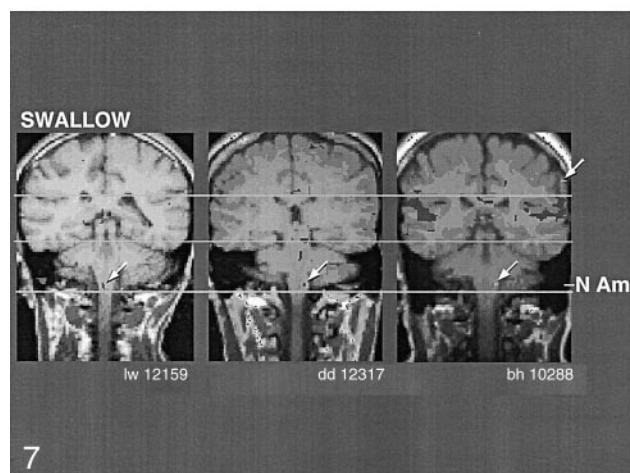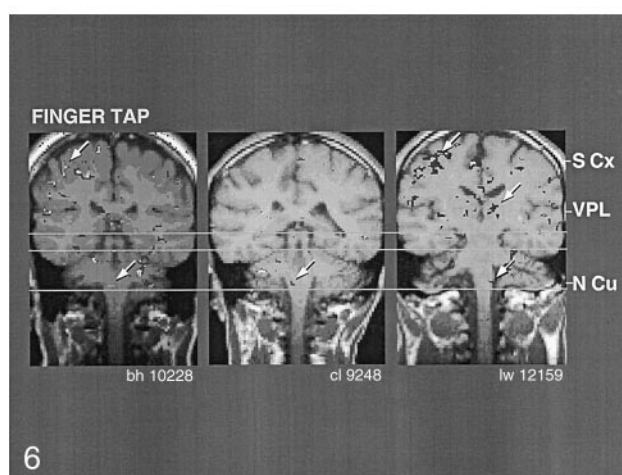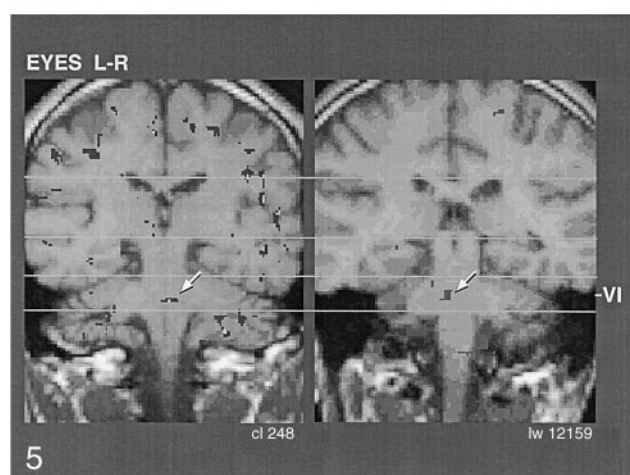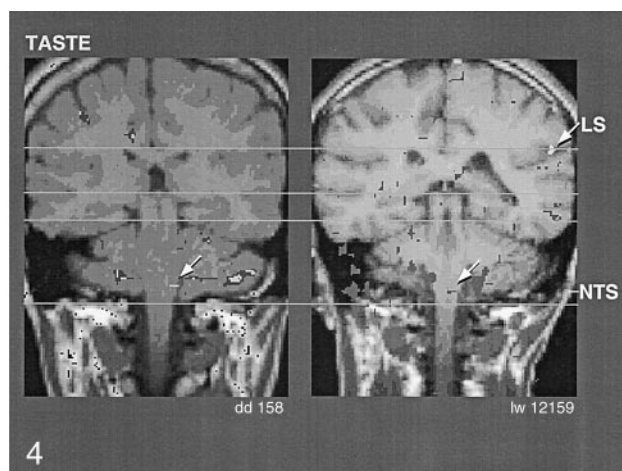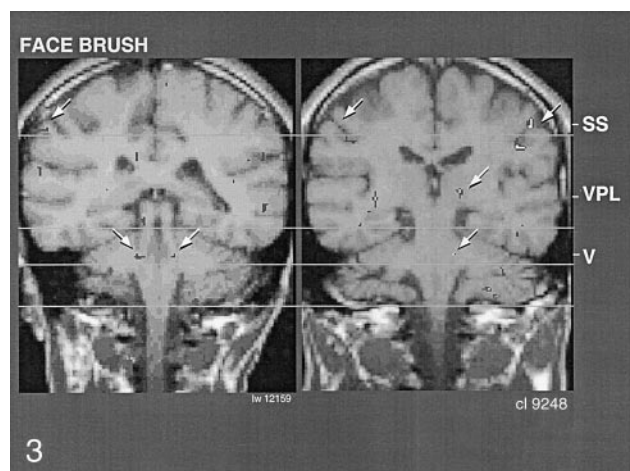
FIG 3. Coronal images show the similarity of activation (*arrows*) produced by brushing the face, which corresponds to the region of the trigeminal main sensory nucleus (*V*), in two individuals. Note activation of nucleus ventralis posteromedialis (*VPL*) in one of the individuals and of somatosensory cortex (*SS*) in both individuals.

FIG 4. Coronal images show the similarity of activation (*arrows*) in the region of the NTS, produced by tasting a sweet-sour-salty-bitter mixture, in two individuals. *LS* indicates the lateral sulcus.

FIG 5. Coronal images shows the similarity of activation (*arrows*) in the region of the abducens nucleus (*VI*), produced by voluntary left-right eye movement, in two individuals.

FIG 6. Coronal images shows the similarity of activation (*arrows*) in the region of the nucleus cuneatus (*N Cu*), produced by tapping the fingers against the thumbs, in three different individuals. Note the activation of the VPL and somatosensory cortex (*S Cx*) in the finger homuncular region as well.

FIG 7. Coronal images shows the similarity of activation (*arrows*) in the region of the nucleus ambiguus (*N Am*) in three individuals. These findings were correlated with dry swallowing (ie, Mendelsohn maneuver).

abducens nucleus is near the midline, whereas the facial nucleus is lateral to it, at about the same level of the neuraxis. Note that the region of BOLD activation in the cortex corresponded to the homuncular region of the face, consistent with the activation in the brainstem. Also shown in Figure 2 is the cross-correlation time series data. The upper part of each of the traces shows the time course of the BOLD signal change in these

ROIs. The lower part shows the time course of the stimulus input; the peak represents the activity of the paradigm, which alternates with the baseline.

Interindividual Regional Reliability

As shown in Figure 3, consistency was observed between the regions of BOLD activation in the pons
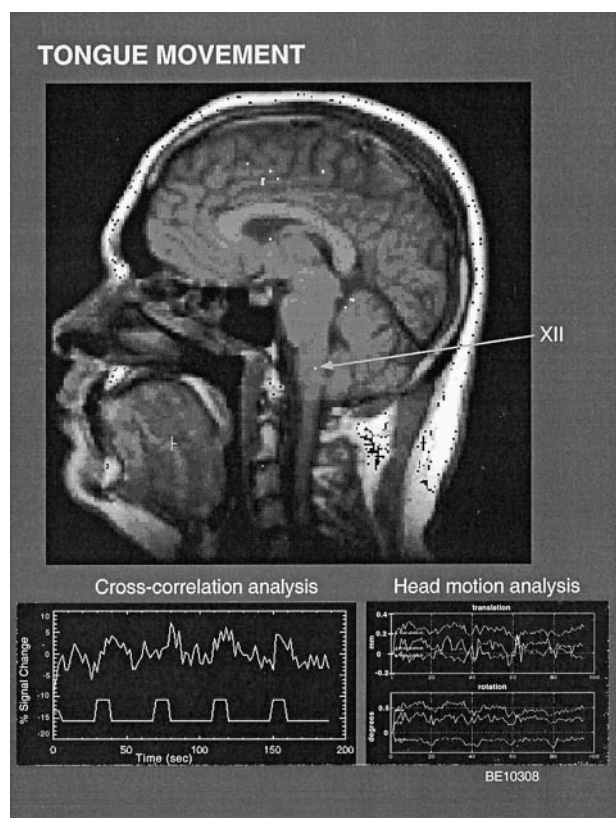
FIG 8. Sagittal view in an individual shows activation in the region of the hypoglossal nucleus (*XII*) and in the muscle of the tongue, in relation to pushing the tongue forcefully and repeatedly against the hard palate. Also shown are the findings from cross-correlation analysis in this region of interest (ROI) and the head movement analysis for this trial. Head movement remained less than 1 mm for the duration of the trial.

and somatosensory cortex in two individuals, in response to brushing of the face. In addition, note the region of BOLD activation in the somatosensory thalamus (ie, VPL) in one of the individuals (*right* image). The triple activation in response to brushing the face was consistent with facial stimulation–induced activation of main trigeminal nucleus of the pons (CN V), VPL of the thalamus, and homuncular facial region of the somatosensory cortex. A probable clinical correlate of these findings of a response to face brushing is the report of cutaneous anesthesia in the maxilla and other facial regions in two cases of a relatively circumscribed lesion in this brain region (26). For bilaterally activated motor or sensory tasks, we often observed only unilateral BOLD activation; this finding was consistent with that of previous reports (19, 20).

Figure 4 shows interindividual consistency in BOLD activation in the region of the superior level of the NTS in the medulla oblongata, in correlation with the taste stimulus. Note the activation of the sensory cortex (*right* image) at the level of the lateral sulcus, which closely corresponded to the homuncular tongue region.

Figure 5 shows interindividual reliability in the region of BOLD activation in correlation with left-to-right eye movement. The pontine location of activation near the midline was consistent with activation of

the abducens nucleus (CN VI). Figure 6 shows that the region of BOLD activation in relation to finger tapping was consistent among three individuals. This finding corresponded to the region of the nucleus cuneatus, which receives afferent activity from the hands. In addition, the region of BOLD activation in the sensory cortex corresponded to the homuncular region for the fingers (note that this region of activation was superior to that in the face in Figure 2). Furthermore, in one subject (*right* image), BOLD activation was evident in the somatosensory thalamus (region of the nucleus VPL); this finding was consistent with afferent activation from the fingers.

Figure 7 shows the BOLD activation pattern that was correlated with dry swallowing (ie, Mendelsohn maneuver). This movement required activation of the nucleus ambiguus of the medulla oblongata. The images show that the region of the nucleus ambiguus was consistently activated in three individuals during the performance of this task. Note the activation at the inferolateral aspect of the motor cortex just superior to the lateral sulcus (*upper arrow*, *right* image), which corresponded to the homuncular pharyngeal region.

Figure 8 is a sagittal view obtained during tongue movement (ie, pushing the tongue forcefully and repetitively against the hard palate). The BOLD activation in a delimited region of the medulla oblongata was highly correlated with the movement, and it was consistent with the location of the hypoglossal nucleus (CN XII). The traces below the brain images show the relation of the time course between the BOLD activity in this ROI and the epochs of tongue movement. The trace at the right side of the image shows the magnitude of head movement, which was less than 1 mm in each of the three axes.

Figure 10 shows BOLD activation in the cervical spinal cord, at the C1, C2 and C3 levels, that were observed in correlation with the tongue movement task. This activation was likely correlated with activity in the motor control of the strap muscles, which stabilize the tongue. The motor neurons that control the strap muscles emerge from these three levels of the spinal cord (5). Also, cortical activation at the level of the homuncular tongue region (near the lateral sulcus) is depicted.

Discussion

Feasibility of Functional Mapping of the Lower Brainstem and Spinal Cord

The present study provides evidence that 1.5-T fMRI can enable localization of the activation of specific CN nuclei and other lower brainstem motor and sensory nuclei, when the movements that those nuclei control are executed or when sensory stimulation to which those nuclei respond is applied. The regions of activation were closely correlated with the known distribution of these nuclei and the motor and sensory functions that they control.

TABLE 1: Summary of responses in specific brain region activation during the performance of the specified paradigms

Paradigm	Region	Subject							Positive Responses	Percentage (%)
		1*	2*	3	4	5	6	7		
Face brushing	CN V sensory	No/yes	No/no	No	No	Yes	Yes	No	3	33
Jaw clenching	CN V motor	Yes/yes	No/yes	No	Yes	No	No	Yes	5	56
L-F eye movement	CN VI	No/yes	No/yes	No	Yes	Yes	No	No	4	44
Smiling, puckering	CN VII	No/yes	Yes/no	No	No	No	Yes	Yes	4	44
Tasting	CN X (NTS)	No/no	No/no	Yes	Yes	Yes	Yes	No	4	44
Tongue tapping	CN XII	No/yes	Yes/yes	No	Yes	No	Yes	Yes	6	67
Swallowing	Nucleus ambiguus	No/yes	Yes/yes	Yes	Yes	Yes	No	Yes	7	78
Finger tapping	Nucleus cuneatus	No/yes	Yes/yes	Yes	Yes	Yes	No	No	6	67
Tongue tapping	C1, C2, C3	Yes/no	No/no	No	No	No	Yes	Yes	3	33

Note.—Each paradigm was applied in each subject.

* Subjects 1 and 2 underwent testing with all paradigms on 2 days. Data are the results of day 1/results of day 2.
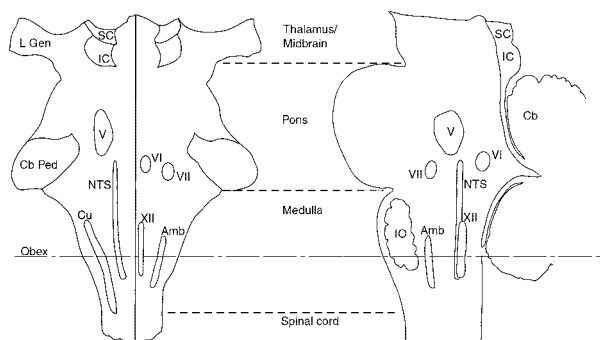

FIG 9. Semi-diagrammatic representation of the location of the lower brainstem nuclei analyzed in the present study, for comparison with fMRI findings (adapted from reference 5, with minor adjustments based on data in reference 2). *Amb* indicates the nucleus ambiguus; *Cb*, cerebellum; *Cb ped*, cerebellar peduncle; *Cu*, nucleus cuneatus; *IC*, inferior colliculus; *IO*, inferior olive; *L Gen*, lateral geniculate nucleus; *NTS*, NTS; *SC*, superior colliculus; *V*, main sensory trigeminal nucleus; *VI*, abducens nucleus; *VII*, facial nucleus; and *XII*, hypoglossal nucleus. For reference, the obex delineates the caudal angle of the rhomboid fossa or fourth ventricle.

Ruling Out Artifacts

We believe that the present findings are not likely to be attributed to motion artifact because of the following: 1) The regions of BOLD activation were closely and differentially related to the location of the motor and sensory nuclei in the pons and medulla oblongata that control the corresponding motor and sensory tasks. 2) Thalamic and cortical regions showed BOLD activation patterns that corresponded to the activation sites in the brainstem. 3) Although different individuals are expected to differ in the strategies that they use to perform the various motor tasks, intersubject reliability of brainstem sites was clearly correlated with the sensory and motor tasks. 4) The magnitude of head movement was less than 1 mm, and the postprocessing method corrected for head movement. 5) The sensory and motor tasks were performed at instantaneous frequencies that were substantially different from, and not temporally correlated with, respiratory and cardiac rhythms. Consequently, any artifact introduced by respiratory and cardiac movements of the brainstem or spinal cord would have occurred in random relation to the move- ments and stimuli under investigation. 6) Artifact produced by respiratory or cardiac movements would have been expected to repeatedly appear across motor and sensory paradigms. However, no such consistent signal was evident in the brainstem in any subject. Consequently, on basis of these six considerations, we believe that systematic motion artifactual error was unlikely to account for the present findings.

Limitations and Advantages of fMRI

A limitation of the present findings is that the fMRI BOLD signal does not provide an exact depiction of the anatomic extent of the brainstem nuclei, but rather, it enables approximate localization. Nevertheless, the method can provide an approximation of the *relative* location of the various nuclei. Thus, the fMRI method could be useful in ascertaining the relative locations of nuclei of interest in specific individuals whose brain sizes and orientation differ idiosyncratically. Thus, the use of fMRI to *functionally locate* a region of interest in a given individual may be more accurate than localization in reference to a histology-based stereotaxic atlas (eg, references 1 and 2) or coordinates based on external landmarks (eg, reference 3).

Because multiple motor and sensory nuclear regions can be functionally mapped in a short period (eg, six to eight regions in 1 hour), triangulation on a selected region of interest by generating a functional reference map in a given individual (eg, as in Fig 2) is feasible. Thereby, the locations of nuclei that surround the region of interest in the lower brainstem can be ascertained.

Potential Clinical Utility of Lower Brainstem Functional Mapping with fMRI

At present, we cannot, with certainty, account for cases in which activation in pons and medulla was not evident despite the performance of vigorous sensory stimulation or voluntary movement that would be expected to activate those regions. This limitation restricts the potential clinical utility of this method at this time, in that the absence of activation cannot be assumed to represent a neurologic dysfunction. On
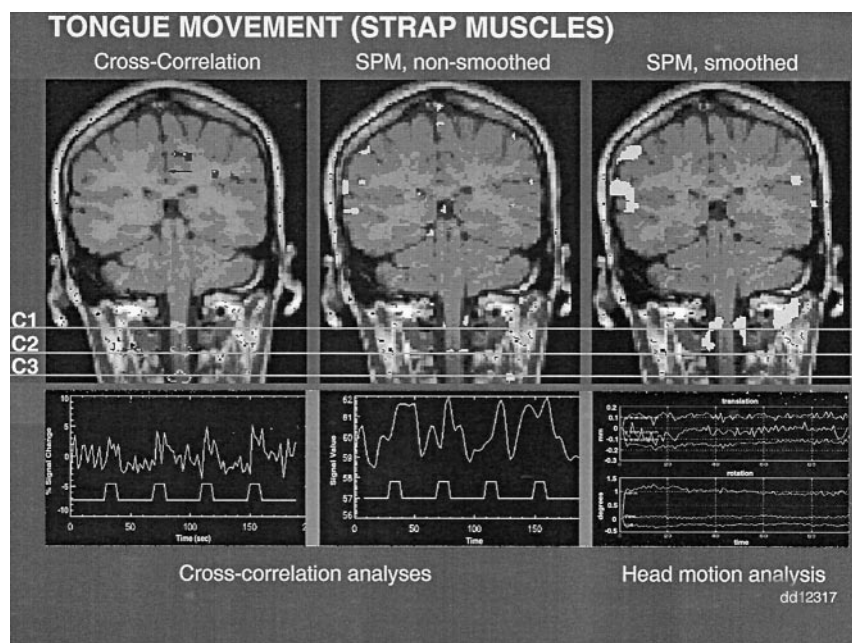
FIG 10. Comparison of cross-correlation analysis and SPM methods with the same data set. The cross-correlation analysis (*top left*) revealed that tongue tapping against the hard palate activated cervical spinal cord regions C1, C2. and C3, which provide the motor innervation of the strap muscles that stabilize the tongue. Similarly, activation of C1 and C2 is shown with the SPM method in its non-smoothed mode (*top middle*), but not in its smoothed mode (*top right*). The unsmoothed SPM analysis revealed a more discrete and delimited localization, more similar to the cross-correlation analysis than the results of smoothed SPM analysis. Findings from cross-correlation (*bottom left, bottom middle*) and head motion analyses (*bottom right*) are also shown. Note also the cortical activation at the level of the homuncular tongue region (near the lateral sulcus, *top middle, top right*).

the other hand, the occurrence of regional activation that corresponds with a specific paradigm could be of potential clinical utility in guiding interventions in which the knowledge of individual idiosyncratic differences in the localization of function is important. Thus, targeting of the facial nucleus (VII) could be facilitated or confirmed by also locating the closely adjacent abducens nucleus (VI) in the same individual; this can be identified by having the individual perform lateral eye movements. This approach could help in locating the critical lower brainstem regions to be avoided during stereotaxic neurosurgical and/or radiosurgical procedures in a particular individual. The proximity of these sites that control facial and lateral eye movement, as observed in the present study (eg, Fig 3), is consistent with the findings in a case report by Hirose et al (11); their patient had combined ipsilateral horizontal gaze paralysis and ipsilateral facial weakness and was found to have a relatively circumscribed ischemic lesion in the related brain region.

As another example, certain nuclear regions of the brainstem tegmentum that are densely vascularized, for example, the hypoglossal and abducens nuclei (41), should be avoided during direct brainstem surgery (eg, puncture and aspiration of cystic tumors) that is performed through safe entry zones via the floor of the 4th ventricle. However, landmarks are not always reliable, as exemplified in a case of the facial colliculus (42). Although the localization of critical brainstem sites can be facilitated by using the statistical triangulation method of Bogucki et al (42), idiosyncratic distortions in the brainstem due to displacement by a tumor could be problematic. Thus, localization of idiosyncratically positioned critical sites could be facilitated by using fMRI to confirm and more precisely specify the location of brainstem nuclei adjacent to the critical sites.

Relation between Cross-Correlation and SPM Analytic Methods

While the cross-correlation analysis and the unsmoothed SPM method provided similar localizations, the smoothed SPM procedure tended to depict large, extended regions of activity that tended to obscure or omit sites that appeared with the other two methods. The relatively good concordance between the cross-correlation and SPM findings, despite their basis on different statistical assumptions, increased the confidence that the activity depicted was not artifactual.

Apparent False-Positive and False-Negative Cases

Note that, in the images, relatively little activity appears in the lower brainstem regions that surround the regions of activation. In those brainstem regions, it was more common for *no* activation to be evident than for activation to be evident in regions that did not correspond to the concurrently performed motor task or sensory stimulation. This finding implies that the present method is conservative, in that any error would be more likely to occur in the direction of a false-negative result (ie, no fMRI evidence of activation in a site, although the site is activated) than a false-positive result (ie, fMRI evidence of activation at a site that is, in actuality, not activated). Consequently, errors, if any, would cause *fewer* regions of activation to be depicted on the image than those actually activated. On the basis of our observations, a lower brain site may likely fail to show activation if the corresponding movement or stimulation is less than vigorous. fMRI instruments with higher sensitivity and resolution will likely increase the reliability of these responses.

Conclusion

With 1.5-T fMRI, the CN nuclei of the pons and medulla and other nuclei of the lower brainstem and cervical spinal cord can be localized in awake humans with the performance of specific motor tasks or sensory stimulation. Thus, functional mapping of the lower brainstem is feasible with this method.

Appendix: Statistical Analysis

SPM Analysis

Statistically significant activation in the sampled volume is determined with the application of a voxel-by-voxel t test, the result of which is transformed to a Z statistic. The resultant map of Z statistics is then displayed on a coregistered high-resolution anatomic MR image (37). The confounding effects of local or regional variation in signal and filtering of noise elements are addressed with spatial smoothing of the image data during the image realignment step (38). Typically, SPM methods use a gaussian smoothing kernel of 8 at full width at half maximum (8 pixels).

Generally, this kernel size is appropriate for cortical areas. However, because the dimensions of the brainstem are considerably less than most cortical areas, a kernel of 8 can either eliminate all of the signal from the brainstem or create a spatially extended area of activation that may cover large regions of the pons and medulla. Therefore, we additionally processed the image data sets without smoothing (ie, unsmoothed method).

To account for hemodynamic delays and to correct for any head motion at the onset of image acquisition, the first eight images are discarded. The remaining images are realigned with the first image of this subtracted series. Image realignment corrects for head motion and permits normalization to a standardized stereotactic coordinate system. Motion correction in image realignment is achieved with the application of a six-parameter affine transformation convolved with time-series elements.

Cross-Correlation Analysis

Motion correction is executed with an in-plane least-squares motion correction algorithm. Spurious signals resulting from motion or cardiac and respiratory cycles are removed by means of a section-wise method that removes spatially coherent signal changes with the application of a partial correlation method to each section in time (39).

The displayed correlation maps are generated with a Fourier transform cross-correlation function that correlates the image time-course intensity change with the stimulus input function on a pixel-by-pixel basis, as follows (Eq 1):

$$1) \quad cc = \frac{\sum_{n=1}^{N}(f_i - u_f)(r_i - u_r)}{\left[\sum_{n=1}^{N}(f_i - u_f)^2\right]^{1/2}\left[\sum_{n=1}^{N}(r_i - u_r)^2\right]^{1/2}},$$

where f_i is the time-course function of a given pixel (for $i = 1$ to N); r_i represents the reference waveform; and u_f and u_r represent the average values of f and r, respectively (40). The time shift at which the correlation is maximum for each pixel was selected for subsequent processing. A two-pixel nearest-neighbor–rule algorithm was incorporated into pixel selection to suppress random-noise contributions to pixel signal. Correlation thresholds for each pixel are set at a probability of .001. The relationship between the probability and the threshold TH is given by Equation 2:

$$2) \quad P = 1 - \frac{2}{\pi^{1/2}}\int_0^{TH\sqrt{N/2}} e^{-t^2}\mathrm{d}t.$$

Probabilities are determined from the complementary error function, errorf (the integral), with the assumption of a gaussian distribution for noise. The P value for a selected pixel at a single time shift for N images and a correlation threshold of cor is determined with Equation 3:

$$3) \quad ef = \mathrm{errorf}\left(\frac{|cor|\sqrt{N}}{\sqrt{2}}\right),$$

where $P = 1 - ef$. Corrected P values for the nearest-neighbor are calculated as follows: $P_{nn} = P_{max} \times [1 - (1 - P_{max})^8$, where $P_{max} = 1 - (efN)$. A Bonferroni correction is applied to the P values of pixels achieving threshold with the α level set at 1500 pixels, as follows (40): $P_{bonferroni} = 1 - (1 - P_{nn})^{1500}$.

The displayed images (128 $\times$ 128 matrix) show pixel dimensions that are smaller than the acquisition pixel dimensions (64 $\times$ 64 matrix). This difference reflects standard resampling algorithms used in the IDL subroutines, that is, rebin and congrid.

Finally, the investigator selects a ROI by circumscribing it with the cursor on the monitor display, and the level of significance of the cross-correlation in that ROI is calculated. Statistical maps of activation are displayed by using a cross-correlation analysis with thresholds set to $R = 0.6$ ($P < .03$). In the present study, all activation sites (ROIs) that are indicated by *arrows* in the accompanying images were found to have a significant correlation ($P < .03$) with the onset and cessation of the motor or sensory tasks.

References

1. Olszewski J, Baxter D. *Cytoarchitecture of the Human Brain Stem.* New York, NY: S. Karger; 1982
2. Paxinos G, Huang XF. *Atlas of the Human Brainstem.* New York, NY: Academic Press; 1995

3. Talairach J, Tournoux P. *Co-Planar Stereotaxic Atlas of the Human Brain.* New York, NY: Thieme Medical Publishers; 1988

4. Krieg WJS. *Functional Neuroanatomy.* 3rd ed. Bloomington, Ind: Pantagraph Printing; 1966

5. Netter FH. *The Ciba Collection of Medical Illustrations. Nervous System: Anatomy and Physiology.* Vol 1. Ciba Pharmaceutical Company, Summit, NJ; 1986:237

6. Szentagothai J, Miklos R. *Funkcionalis anatomia.* Budapest, Hungary: Semmelweis Kiado; 1994

7. Heimer L. *The Human Brain and Spinal Cord.* New York, NY: Springer-Verlag; 1994

8. Nieuwenhuys R, Voogd J, van Huijzen C. *The Human Central Nervous System.* New York, NY: Springer-Verlag; 1983

9. Solsberg MD, Fournier D, Potts DG. **MR imaging of the excised human brainstem: a correlative neuroanatomic study.** *Am J Neuroradiol* 1990;11:1003–1013

10. Flannigan BD, Bradley WG Jr, Mazziotta JC, et al. **Magnetic resonance imaging of the brainstem: normal structure and basic functional anatomy.** *Radiology* 1985;154:375–383

11. Hirose G, Furui K, Yoshioka A and Sakai K. **Unilateral conjugate gaze palsy due to a lesion of the abducens nucleus: clinical and neuroradiological correlations.** *J Clin Neuroophthalmol* 1993;13:54–58

12. Muri RM, Chermann JF, Cohen L, Rivaud S, Pierrot-Deseilligny C. **Ocular motor consequences of damage to the abducens nucleus area in humans.** *J Neuroophthalmol* 1996;16:191–195

13. Edwards MS, Wara WM, Ciricillo SF, Barkovich AJ. **Focal brainstem astrocytomas causing symptoms of involvement of the facial nerve nucleus: long-term survival in six pediatric cases.** *J Neurosurg* 1994;80:20–25

14. Wortham DG, Teresi LM, Lufkin RB, Hanafee WN, Ward PH. **Magnetic resonance imaging of the facial nerve.** *Otolaryngol Head Neck Surg* 1989;101:295–301

15. Corfield DR, Murphy K, Josephs O, et al. **Cortical and subcortical control of tongue movement in humans: a functional neuroimaging study using fMRI.** *J Appl Physiol* 1999;86:1468–1477

16. Lee SS, Wang SJ, Fuh JL, Liu HC. **Transient unilateral hypoglossal nerve palsy: a case report.** *Clin Neurol Neurosurg* 1994;96:148–151

17. Takimoto T, Saito Y, Suzuki M, Nishimura T. **Radiation-induced cranial nerve palsy: hypoglossal nerve and vocal cord palsies.** *J Laryngol Otol* 1991;105:44–45

18. Brown JW. **Prenatal development of the human nucleus ambiguus during the embryonic and early fetal periods.** *Am J Anat* 1990;189:267–283

19. Hartmann HA, McMahon S, Sun DY, Abbs JH, Uemura E. **Neuronal RNA in nucleus ambiguus and nucleus hypoglossus of patients with amyotrophic lateral sclerosis.** *J Neuropathol Exp Neurol* 1989;48:669–673

20. Mosier K. **Functional MRI of swallowing.** In: Mukherji S, Castelijns J. *Modern Head and Neck Imaging.* Berlin, Germany: Springer-Verlag; 1999:79–86

21. Mosier KM, Liu WC, Maldjian JA, Shah R, Modi B. **Lateralization of cortical function in swallowing: a functional MR imaging study.** *Am J Neuroradiol* 1999;20:1520–1526

22. Mosier K, Patel R, Liu WC, Kalnin A, Maldjian J, Baredes S. **Cortical representation of swallowing in normal adults: functional implications.** *Laryngoscope* 1999;109:1417–1423

23. Lazarus C, Logemann JA, Gibbons P. **Effects of maneuvers on swallowing function in a dysphagic oral cancer patient.** *Head Neck* 1993;15:419–424

24. Kahrilas PJ, Logemann JA, Krugler C, Flanagan E. **Volitional augmentation of upper esophageal sphincter opening during swallowing.** *Am J Physiol* 1991;260:G450–G456

25. Hamdy S, Mikulis DJ, Crawley A, et al. **Cortical activation during human volitional swallowing: an event-related fMRI study.** *Am J Physiol* 1999;277:G219–G225

26. Kiers L, Carroll WM. **Blink reflexes and magnetic resonance imaging in focal unilateral central trigeminal pathway demyelination.** *J Neurol Neurosurg Psychiatry* 1990;53:526–529

27. Onoda K, Ikeda M. **Gustatory disturbance due to cerebrovascular disorder.** *Laryngoscope* 1999;109:123–128

28. Lee BC, Hwang SH, Rison R, Chang GY. **Central pathway of taste: clinical and MRI study.** *Eur Neurol* 1998;39:200–203

29. Imaiso Y, Taniwaki T, Yamada T, Kira J, Kobayashi T. **Myelopathy due to vitamin B12 deficiency presenting only sensory disturbances in upper extremities: a case report.** *Rinsho Shinkeigaku* 1997;37:135–138

30. Hsieh CL, Shima F, Tobimatsu S, Sun SJ, Kato M. **The interaction of the somatosensory evoked potentials to simultaneous finger stimuli in the human central nervous system: a study using direct recordings.** *Electroencephalogr Clin Neurophysiol* 1995;96:135–142

31. Florence SJ, Wall JT, Kaas JH. **Somatotopic organization of inputs from the hand to the spinal gray and cuneate nucleus of monkeys with observations on the cuneate nucleus of humans.** *J Comp Neurol* 1989;286:48–70

32. Han JS, Bonstelle CT, Kaufman B, et al. **Magnetic resonance imaging in the evaluation of the brainstem.** *Radiology* 1984;150:705–712

33. Ormerod IE, Bronstein A, Rudge P, et al. **Magnetic resonance imaging in clinically isolated lesions of the brain stem.** *J Neurol Neurosurg Psychiatry* 1986;49:737–743

34. Fasano FJ Jr, Stauffer ES. **Traumatic division of the spinal cord demonstrated by magnetic resonance imaging: report of two cases.** *Clin Orthop* 1988;233:168–170

35. Stroman PW, Nance PW, Ryner LB. **BOLD MRI of the human cervical spinal cord at 3 tesla.** *Magn Reson Med* 1999;42:571–576

36. Ogawa S, Lee TM, Kay AR, Tank DW. **Brain magnetic resonance imaging with contrast dependent on blood oxygenation.** *Proc Natl Acad Sci U S A* 1990;87:9868–9872

37. Friston K. **Statistical parametric mapping and other analyses of functional imaging data.** In: Toga AM JC, eds. *Brain Mapping: The Methods.* New York, NY: Academic Press; 1996:363–386

38. Poline JB, Holmes A, Worsley K, Friston KJ. **Making statistical inferences.** In: Frackowiak RSJ, Friston KJ, Frith CD, Dolan RJ, Mazziotta JC. *Human Brain Function.* New York, NY: Academic Press; 1997:85–106

39. Zarahn E, Aguirre GK, D'Esposito M. **Empirical analyses of BOLD fMRI statistics. I. Spatially unsmoothed data collected under null-hypothesis conditions.** *Neuroimage* 1997;5:179–197

40. Maldjian J, Atlas SW, Howard RSI, et al. **Functional magnetic resonance imaging of regional brain activity in patients with intracerebral arteriovenous malformations before surgical or endovascular therapy.** *J Neurosurg* 1996;84:477–483

41. Duvernoy HM. *Human Brain Stem Vessels.* New York, NY: Springer-Verlag; 1978

42. Bogucki J, Gielecki J, Czernicki Z. **The anatomical aspects of a surgical approach through the floor of the fourth ventricle.** *Acta Neurochir (Wien)* 1997;139:1014–1019